GLOBAL CHANGE BIOLOGY
BIOENERGY

GCB Bioenergy (2015) **7**, 774–784, doi: 10.1111/gcbb.12169

Forecasting changes in water quality in rivers associated with growing biofuels in the Arkansas-White-Red river drainage, USA

HENRIETTE I. JAGER[1], LATHA M. BASKARAN[1], PETER E. SCHWEIZER[1], ANTHONY F. TURHOLLOW[1], CRAIG C. BRANDT[1] and RAGHAVAN SRINIVASAN[2]

[1]*Oak Ridge National Laboratory, Oak Ridge, TN, 37831-6036, USA,* [2]*Texas A&M University, College Station, TX, USA*

Abstract

Excess nutrients from agriculture in the Mississippi River drainage, USA have degraded water quality in freshwaters and contributed to anoxic conditions in downstream estuaries. Consequently, water quality is a significant concern associated with conversion of lands to bioenergy production. This study focused on the Arkansas-White-Red river basin (AWR), one of five major river basins draining to the Mississippi River. The AWR has a strong precipitation gradient from east to west, and advanced cellulosic feedstocks are projected to become economically feasible within normal-to-wet areas of the region. In this study, we used large-scale watershed modeling to identify areas along this precipitation gradient with potential for improving water quality. We compared simulated water quality in rivers draining projected future landscapes with and without cellulosic bioenergy for two future years, 2022 and 2030 with an assumed farmgate price of $50 per dry ton. Changes in simulated water quantity and quality under future bioenergy scenarios varied among subbasins and years. Median water yield, nutrient loadings, and sediment yield decreased by 2030. Median concentrations of nutrients also decreased, but suspended sediment, which is influenced by decreased flow and in-stream processes, increased. Spatially, decreased loadings prevailed in the transitional ecotone between 97° and 100° longitude, where switchgrass, *Panicum virgatum L.*, is projected to compete against alternative crops and land uses at $50 per dry ton. We conclude that this region contains areas that hold promise for sustainable bioenergy production in terms of both economic feasibility and water quality protection.

Keywords: bioenergy, biofuels, cellulosic feedstocks, land-use change, *Panicum virgatum*, POLYSYS, Soil Water Assessment Tool, sustainability, water quality

Received 5 December 2013 and accepted 3 January 2014

Introduction

Historical shifts in land use and land cover have caused, and may continue to cause, large-scale shifts in the health of rivers and streams of the Great Plains region of the United States. Historically, water quality in rivers of the Great Plains was impacted by conversion from a landscape of native prairie maintained by fire to a landscape dominated by human agriculture interspersed with urban centers (Dodds & Oakes, 2004). Less than 1% of the original tallgrass prairie in North America remains (Samson & Knopf, 1994; Kiniry *et al*., 2005). This large-scale conversion into agriculture resulted in elevated nutrient and sediment loads in streams of the Arkansas-White-Red (AWR) river basin, which drains the southern portion of the Great Plains (Johnson *et al*., 1997; Alexander & Smith, 2006; Harmel *et al*., 2006). The AWR river basin drains into the lower Mississippi River and contributes nutrients that combine with loadings from other river basins to cause large areas of hypoxia in the Gulf of Mexico (Gelfand *et al*., 2013). This 'dead' zone continues to have significant economic impacts on fisheries in the Gulf of Mexico.

Over the past few decades, the nutrient status of rivers draining agricultural lands in the Great Plains has improved for two reasons: First, the amount of agricultural land has stabilized (Parton *et al*., 2007). Second, The Clean Water Act (33rd United States Congress §1251 et seq. 1972) required treatment of waste water and other point sources (Alexander & Smith, 2006). Nevertheless, nonpoint agricultural nutrient contributions continue to degrade surface water quality. For example, nitrate concentrations are higher in streams draining lands with a higher percentage of land planted in agricultural crops than in streams with lower percentages (Dodds & Oakes, 2008). AWR subbasins with recent impaired water listings under §303 of the Clean Water Act are shown in Fig. 1.

Correspondence: Henriette I. Jager, tel. 865-574-8143, fax 37831-6038, e-mail: jagerhi@ornl.gov

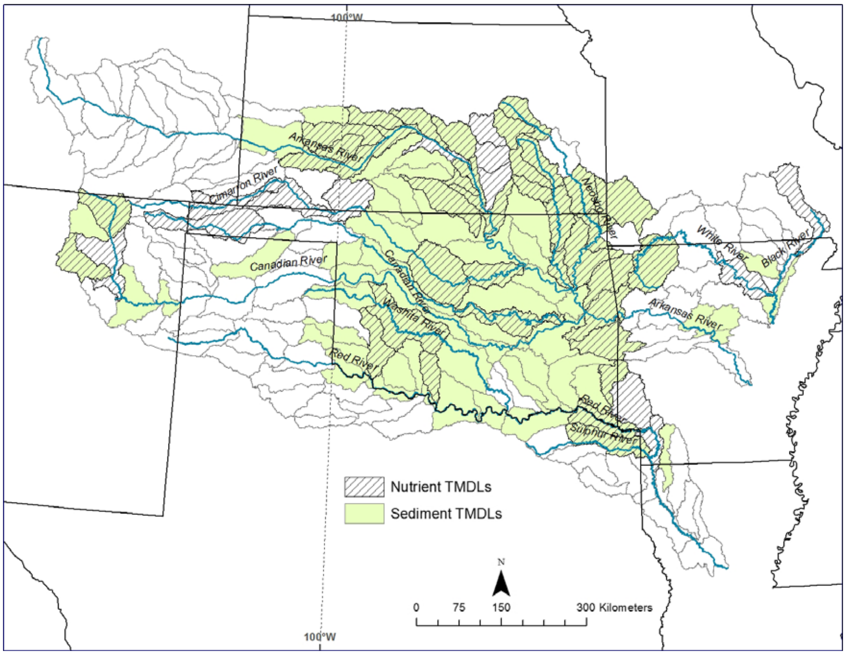

Fig. 1 Geographic distribution of subbasins with waters listed as impaired by the USEPA under §303d due to nutrient and/or sediment water quality violations. Data are for years 2004, 2006, 2008. The 100th meridian is shown, demarking the transition from areas that require irrigation (<20 inches precipitation) to the west and areas that do not require irrigation to the east.

Landscapes of the Great Plains are now facing another large shift in land use. The Energy Independence and Security act of 2007 set a target for US cellulosic-ethanol production of 60.6-billion liters by 2022. Shifting from fossil fuels to required levels of cellulosic-ethanol will require large-scale conversion, or more-intensive use, of lands that are currently serving other purposes. Because land use has a large influence on water quality (Hunsaker & Levine, 1995; Allan, 2004), widespread crop replacements will likely alter the water quality of US rivers. Corn grain is currently the dominant feedstock for ethanol produced in the United States (Larson *et al.*, 2008), and increased corn production for ethanol and for food have similar adverse water quality impacts. Donner & Kucharik (2008) estimated that meeting a target of 56.8–136.3 billion liters of fuel produced from corn would increase the annual flux of dissolved inorganic nitrogen by 10–36% and make it nearly impossible to meet targets for reducing hypoxia in the Gulf of Mexico.

However, the AWR river basin may be one region that can grow bioenergy feedstocks sustainably. The drier western half of the AWR basin is better suited for growing crops such as winter wheat and hay than corn. This basin also has high potential for growing dedicated perennial bioenergy feedstocks such as switchgrass, *Panicum virgatum L.* (U.S. Department of Energy, 2011). In some areas, switchgrass could be grown without irrigation, replacing row crops that would require irrigation from the Ogallala aquifer, which is being depleted by withdrawal rates that exceed recharge rates (Musick *et al.*, 1990; Scanlon *et al.*, 2012).

The purpose of this study was to project future changes in water quality following conversion of lands to grow feedstocks including corn stover and dedicated cellulosic feedstocks. We projected future land-use changes using an economic model and simulated crop growth and water quality in rivers using the Soil Water Assessment Tool (SWAT) (Gassman *et al.*, 2007; Srinivasan *et al.*, 2010). We forecasted changes in water quantity and quality for two future scenarios, 2022 and 2030, consistent with targets for producing second-generation cellulosic biofuels specified by the U.S. Department of Energy (2011).

Materials and methods

Our approach compared water quality in rivers draining landscapes with and without bioenergy crops. Water quality was predicted by the SWAT model, and for each landscape, we averaged results over 20 years to represent variation in climate. Thus, even though we use the terms 'prebioenergy' and 'postbioenergy' landscapes, our SWAT simulations are intended to capture (i.e. average over) interannual climate variation, and not to actually predict year-to-year changes in water quality.

Previously, Baskaran *et al.* (2010) conducted a sensitivity analysis to identify parameters influencing flow for two subbasins in the AWR, followed by calibration of those parameters. In addition, measured and predicted flows were related

(R^2 = 0.83) on a monthly timescale across 173 subbasins of the AWR (Baskaran *et al.*, 2010).

Below we describe our methods for representing landscapes and the watershed modeling.

Future landscapes with and without cellulosic bioenergy

For the initial landscape, we adopted the 2009 Crop Data Layer (CDL-09) (USDA National Agricultural Statistics Service Cropland Data Layer 2009) with land uses aggregated to be consistent with those used to project future landscapes including bioenergy crops and stover (Fig. 2a). In addition, we evaluated a scenario without bioenergy that included the same assumptions about tillage and yield improvements, but without adding bioenergy crops to the landscape or harvesting stover.

Future landscapes that included cellulosic bioenergy (CB) were produced by downscaling county-level forecasts from an economic forecasting model (POLYSYS) for the agricultural sector of the US economy (De La Torre Ugarte & Ray, 2000). According to Langholtz *et al.* (2012), POLYSYS can be conceptualized as an equilibrium displacement model with a system of interdependent modules that simulate (i) crop supply for each of 3110 independent US counties, (ii) crop demands and

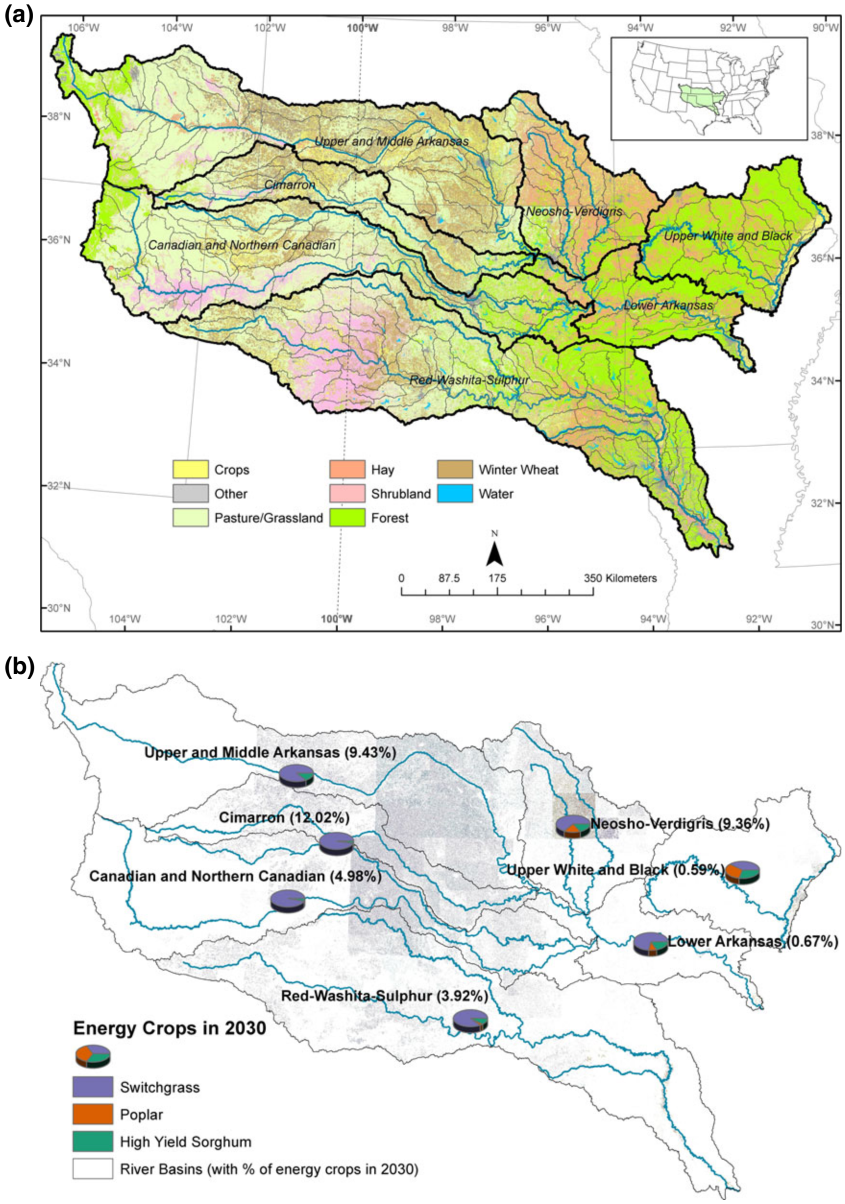

Fig. 2 Maps showing the distribution of land use categories (a) for a no-cellulosic bioenergy (CB) 2009 land cover and (b) for a future 2030 projected land cover (CB-2030). Future land cover including cellulosic biofuels were predicted and downscaled for the CB-2030 scenarios by the Billion-Ton Update.

prices, (iii) livestock supply and demand, and (iv) agricultural income. The crop supply modules are driven by planted and harvested area for major crops (corn, grain, sorghum, oats, barley, wheat, soybeans, cotton, rice, and hay), livestock, food, and feed markets. Based on land rents, POLYSYS forecasted future changes in cropland allocated to major agricultural and energy crops. In the AWR region, dedicated energy crops included switchgrass, poplar, and high-yield sorghum. Dedicated energy crops replaced current land uses in the landscape wherever they produced a higher profit, with some constraints added (U.S. Department of Energy, 2011). One constraint uses allocation rules to limit the cropland area that can switch to simulate the inelastic nature of agricultural supply. Another constraint requires loss of regional forage production associated with livestock to be replaced through intensification of an equal amount of regional pastureland (Langholtz *et al*., 2012). Initial conditions were anchored to USDA baseline economic projections.

We selected two future scenarios, 2022 and 2030, with an assumed price 'at the farm gate' for all bioenergy feedstocks of \$50/dry ton and, following the USDA baseline projections, an assumed annual yield increase of 1% [scenario #73 in U.S. Department of Energy (2011)]. We developed a stochastic Markov model for allocating projected land-use changes to reasonable CDL land-cover categories using county-level transition probabilities. Transition probabilities were estimated from interannual changes in crop area produced by the POLYSYS model. Final categories assigned to 56-m pixels resulted from multiplying successive transitions between specified years. For the CB scenarios, we calculated transition probabilities between 2009 and two future years, 2022 and 2030. We then applied these change probabilities to the each pixel in the 2009 CDL to create a landscape realization for 2022 and 2030. Note that changes in economic forecasts for conventional crops resulted in some changes in area occupied by these crops (i.e. not all changes are due to introduction of bioenergy crops), but these changes are relatively minor.

Watershed modeling

Hydrologic response units. We implemented SWAT for 173 subbasins (USGS 8-digit-HUCs) within the AWR drainage. Delineation of watersheds and hydrography is described in Baskaran *et al.* (2010). We used spatial layers describing soils, slope (from elevation), and land cover to partition each subbasin into areas with similar Hydrologic responses (HRUs) to climate. These nonspatial HRUs are the fundamental unit modeled by SWAT.

Hydrologic responses represented unique combinations of three attributes: soil type, slope, and land use or land cover. STATSGO soil map units (Soil Survey Staff, 1994) that comprised more than 10% of a subbasin were retained. Maloney *et al.*, (2005a,b) showed that disturbances had greater impacts on sediment loadings in streams for watersheds with slopes greater than 5%. We therefore discretized slope into three categories, <2%, 2–5%, and >5%. Because a small amount of steep land can have large effects on sediment losses, we included all slope categories, regardless of the amounts present. Defining land-use categories for HRU construction required that we cross-reference SWAT land-use classes with CDL-09 classes (corn, cotton, forest, hay, oats, pasture/grassland, rangeland, rice, sorghum, soybeans, water, wetland, and winter wheat) and managed agricultural classes modeled by POLYSYS, the economic model. We retained land-use classes that comprised more than 5% of the subbasin. This protocol resulted in a total of 11 225 distinct HRU's. Land use in future landscapes was assigned to the same categories as the CDL-09, but in different places and amounts.

Climate. Because the hydrologic model is sensitive to local precipitation, we used climate data from DAYMET (Thornton *et al.*, 1997) estimated for the center of each subbasin over the period 1980–2011. Daily climate variables included were total precipitation (mm), minimum and maximum temperatures (°C), and solar radiation (MJ m^{-2} d^{-1}). Three other variables (wind speed, relative humidity, and potential evaporation) were simulated by the SWAT model's climate generator (Gassman *et al.*, 2007; Srinivasan *et al.*, 2010).

Management of conventional crops. Conventional agricultural land uses dominant in this region are wheat, hay, corn, and pasture. Below, we describe refinements in management (planting and harvest) of these crops over the defaults reported by (Baskaran *et al.*, 2010). In particular, we describe our management assumptions about fertilizer application, stover removal, and tillage, for future scenarios with and without cellulosic bioenergy.

We simulated planting and plant growth using the heat units scheduling approach, where the required heat units were determined from historical climate data and reported planting dates in Texas and Kansas (U.S. Department of Agriculture, 1997; Baskaran *et al.*, 2013). Annual crops were harvested after accumulating 120% of heat units to reach maturity; this allowed biomass to dry prior to harvest.

Winter wheat was modeled as a winter crop with planting in fall and harvest the next spring or summer. We calculated potential heat units accumulated for planting and harvest using the usual planting and harvest dates for winter wheat. Between spring harvest and fall planting, only crop residue remained on the ground and the parameter controlling the relationship between precipitation and runoff ('curve number' or CN) was increased to represent bare ground. After planting, the curve number reverted to that for cultivated winter wheat.

We treated both grassland hay and pasture hay as perennial crops with 'harvest only' operations simulated for 9 years followed by harvest-and-kill operations during the end of the 10th year and planting after the 10th year. Harvest of hay was simulated three times per year and 90% of the aboveground biomass was cut during each harvest. Twenty percent of the harvested biomass remained as residue. We simulated conventional tillage for the first 9 years, but not the 10th. During the 10th year, we simulated two harvest-only operations and a final harvest-and-kill operation. In future scenarios, we simulated stover removal for corn and wheat up to 80% of aboveground biomass.

Tillage. Tillage practices have been shifting from conventional to no-till over the past decades, and this trend is likely to continue (Uri, 2000; Horowitz *et al*., 2010). In both No-CB and CB scenarios, we assumed a 1.5% increase in land allocated to no-till each year. Half of area of land converted to no-till was removed from land managed using conventional till and the other half from land managed using reduced till. We used a time-for-space substitution to simulate spatial variation in tillage by simulating three tillage practices during different years of a rotation. Knowing the proportions of land, pT_i in three tillage categories, i = 1,2,3 (no till, reduced till, and conventional till), we selected the rotation period for each crop that minimized integer truncation error, i.e. $\min_R \sum[(pT_i \times R) - \text{floor}(pT_i \times R)]$, $R = 3,\ldots,10$. We then apportioned years among the three tillage practices according to proportions pT.

Irrigation and fertilizer application. We simulated irrigation of corn in drier portions of the AWR using SWAT's autoirrigation. When water stress reduced growth by 7.5%, irrigation was simulated by drawing water from a shallow aquifer (the Ogallala) in the same subbasin. Fertilizer application was simulated by crop. Crop-specific hypothetical fertilizers, based on USDA-reported N : P ratios, were applied up to an annual limit whenever nutrient stress reduced crop growth by 25%. We calibrated upper limits on nitrogen fertilizer amounts for wheat, hay, soybeans, corn, and sorghum by comparing simulated amounts with reported fertilizer use (U.S. Department of Agriculture, 2009). Pasture fertilization by manure was estimated using county-level statistics on cattle numbers (Baskaran *et al*., 2013).

Management of energy crops and stover. Modifications to growth and management parameters were required to represent perennial energy crops, as described in Table 1. Energy crops included in CB simulations of 2022 and 2030 were switchgrass, poplar, and high-yield sorghum. No irrigation was simulated for these crops. We simulated an 8-year poplar rotation based on assumptions of the Billion-Ton update (U.S. Department of Energy, 2011). Our growth parameters for energy sorghum, an annual cellulosic feedstock, were derived from USDA crop data (White, 2006; Venuto & Kindiger, 2008; Erickson *et al*., 2012).

We simulated a 10-year switchgrass rotation (U.S. Department of Energy, 2011). During establishment (first 2 years), we simulated a harvest operation with a harvest efficiency of 0.8 and applied only phosphate (44.8 kg P ha^{-1}). During subsequent years, we began with switchgrass already planted and ended the growing season with a harvest-only operation. In nonestablishment years, we simulated nitrogen application when plants became stressed (25% reduced growth, 87.4 kg ha^{-1} N maximum). Averaged over simulated years, this resulted in simulated annual fertilizer applications of between 10.3 to 47.5 kg ha^{-1} N and a median of 18.3 kg ha^{-1} N (Baskaran *et al*., 2013). Spatially, fertilizer amounts followed the precipitation gradient, with higher values in the east. We represented seasonal translocation of nitrogen by varying the aboveground concentrations in switchgrass at emergence (0.0064 kg N kg^{-1}), 50% maturity (0.0044 kg N kg^{-1}), and maturity (0.003 kg N kg^{-1} biomass), based on field trials in west Tennessee (Garten *et al*., 2011). We assumed that the fraction of N in yield was 0.003 kg N kg^{-1} biomass.

We adopted the SWAT-default for aboveground concentration of 0.0022 kg kg^{-1} biomass for phosphorus, which is well supported (Sanderson *et al*., 2001; Clark *et al*., 2005). According to Flueck *et al*. (2011), switchgrass removes about 4.55 kg of P per metric ton. Runoff curve numbers used for switchgrass were 31, 59, 72, and 79, for four hydrologic soil categories ranging from well-drained to poorly drained soils (Arnold *et al*., 2012). We assumed a maximum rooting depth of 2.2 m (Kiniry *et al*., 2005). Each year, switchgrass required 1358.2 physiological heat units to reach maturity. Literature values vary from 1100 at higher latitudes to 2300 in Texas (Kiniry *et al*., 1996). We simulated harvest after reaching 1.2 × heat units required to reach maturity. This allowed for crop drying. We assumed that 90% of the aboveground biomass was cut each year with a harvest efficiency of 80%, with the remainder left as residue.

Simulated water quality and quantity

We simulated and compared precellulosic bioenergy (No-CB-2022 and No-CB-2030) and postcellulosic bioenergy (CB-2022 and CB-2030) scenarios using the same assumptions, consistent

Table 1 Summary of simulated crop management precellulosic bioenergy (No-CB) and postcellulosic bioenergy (CB) scenarios that assumed \$50 dry ton^{-1} farmgate price and 1% annual increase in yield upon replanting

Crop type	No-CB scenario	CB scenarios
Switchgrass	None planted	10-year rotation autofertilized up to 87.4 kg ha^{-1} yr^{-1} N from year 3; 44.8 kg ha^{-1} yr^{-1} P
Poplar	None planted	8-year rotation autofertilized up to 100.9 kg ha^{-1} yr^{-1} N in year 3 & 6; 16.8 kg ha^{-1} yr^{-1} P in year 3
Hi-yield sorghum	None planted	Autofertilized up to 168.1 kg ha^{-1} yr^{-1} N; 67.2 kg ha^{-1} yr^{-1} P
Row crops	No stover removal Higher%no-till Corn irrigated when experiencing water stress	Stover removal Higher%no-till Corn irrigated when experiencing water stress
Hay	Autofertilized up to 224 kg ha^{-1} yr^{-1} 3-cut harvest	Autofertilized up to 224 kg ha^{-1} yr^{-1} 3-cut harvest
Winter wheat	Autofertilized up to 64.6 kg N ha^{-1} yr^{-1} planted in fall harvested in spring no stover removal	Autofertilized up to 64.6 kg N ha^{-1} yr^{-1} planted in fall harvested in spring stover removal up to 80%
Pasture	Cattle grazing fertilized by manure	No intensification, compaction fertilized by manure

with those of the Billion-Ton update, for future tillage and yield increases for No-CB scenarios as well as CB scenarios. Thus, a different No-CB scenario was required for each future year. This enabled us to separate and focus on the effect of growing energy crops and not changes over time. For each scenario, we used SWAT to simulate 30 years of climate based on historical data (treated as replicates), with the first 10 (1-switchgrass rotation) treated as spin-up years and removed from analysis.

We calculated percent change between simulated water quality results for CB and no-CB future scenarios. We constructed a distribution of changes comprised of responses of 173 subbasins to 22 years of climate. We report the 25th, 50th (median), and 75th percentile of the distribution of percent changes in subbasin-area-weighted loadings (kg ha^{-1}) and concentrations (mg L^{-1}) of nitrate (NO3), total nitrogen (TN), phosphate (PO4), and total phosphate (TP). For sediment, changes in loading (sediment yield, SYLD) and concentration (total suspended sediment, TSS) are reported. For water, we report both the flow at subbasin outlets and the water yield (WYLD) in units of cms (converted from mm).

Results

Below, we present results of POLYSYS forecasting, SWAT calibration results for hydrology and nutrients, and predictions for future water quality and water quantity under projections for each of two future years.

POLYSYS future landscapes

In this river basin, switchgrass was forecasted to be the main energy crop (Fig. 2b). Switchgrass acreage increased to represent about 3.8% of the landscape in 2022 and 5.1% in 2030 (Fig. 3). The largest declines were in wheat, hay, and pasture. A small amount of energy sorghum and poplar was also expected to enter the agricultural landscape. Overall, the distribution of bioenergy yields in the CB-2030 scenario averaged 8.63 Mg ha^{-1}. The distribution over all subbasins is shown in Fig. 4.

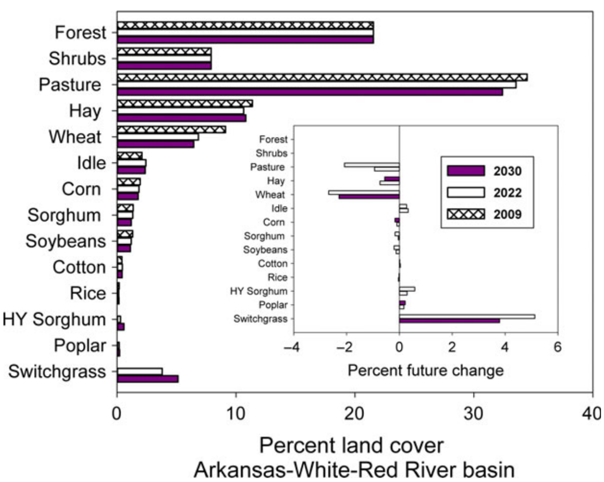

Fig. 3 Percent area for natural landuse/cover categories, agricultural and bioenergy crops for the No-CB-2009 scenario and for future projections for 2022 and 2030.

Water quality futures

We observed a wide range of responses to conversion of lands to bioenergy crops, as measured by the distribution of changes in simulated water quality indicators over 173 subbasins and multiple years. Although variability among river basins was high, we observed shifts in the direction of decreased nutrient loads and water yields by 2030, as described below. Median concentrations of TSS increased by a small percentage, whereas median loadings decreased by a larger percent (Fig. 5).

Future 2022. Compared with the no-CB-2022 scenario, simulated area-weighted nutrient and sediment loadings in simulated CB-2022 landscapes decreased to a greater extent than outlet concentrations (Table 2). Nitrate concentrations increased in 60% of subbasins, with a median change of +4% (+0.03 mg L^{-1}), whereas loadings decreased in 65% of subbasins with a median change of −19.2% (−0.08 kg ha^{-1}). Concentrations of TN increased in 55% of subbasins, with a median change of 8.2% (0.004 mg L^{-1}), whereas loadings decreased in 70% of subbasins with a median change of −19.3% (−0.35 kg ha^{-1}). For phosphorus, both concentrations and loadings decreased in 75% of subbasins. The median change in TP concentration was −1.6% (−0.086 mg L^{-1}) and the median change in loading was −21.6% (−0.14 kg ha^{-1}).

Average flow decreased at the outlets of 85% of subbasins, with a median change of −10.3% (−79.4 m^3 s^{-1}).

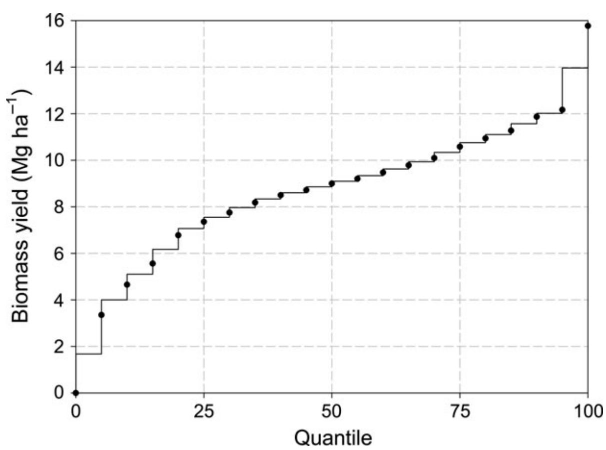

Fig. 4 Cumulative frequency distribution of total bioenergy yields for the 2030 future cellulosic bioenergy (CB) scenario.

TSS concentrations increased in 60% of subbasins and showed a median change of +1.96% (8.07 mg L^{-1}), but loadings decreased in 80% of subbasins, with a median change of −28.9% (−86.3 kg ha^{-1}).

When weighted by area planted in bioenergy crops, median annual nutrient and sediment loadings for CB-2022 decreased from those produced by corresponding No-CB landscapes for all analytes: −0.114 kg ha^{-1} NO3; −1.2 kg TN ha^{-1}; −0.51 kg TP ha^{-1}; −146.5 kg sediment ha^{-1}. Median water yield decreased by 21.8%. For reference, median annual loadings weighted by total subbasin area for the No-CB-2022 scenario were 0.722 kg ha^{-1} NO3, 3.620 kg TN ha^{-1}, 0.752 kg TP ha^{-1}, 373.7 kg sediment ha^{-1}, and 3,757 m^3 s^{-1} water.

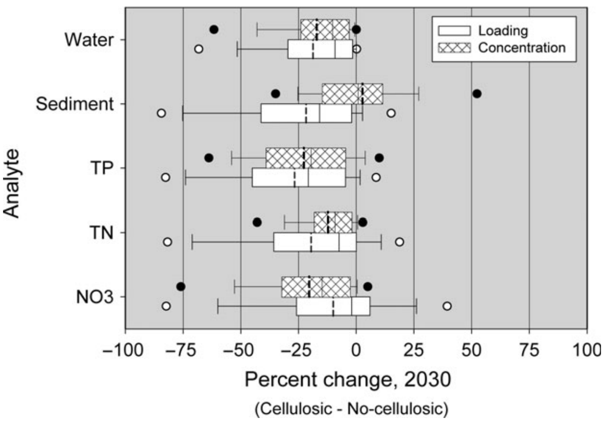

Fig. 5 Box-whisker diagram of percent changes in subbasin-area-weighted loadings (open bar) and outlet concentrations (cross-hatch) between future cellulosic bioenergy (CB) scenarios for 2030 and the corresponding scenario without cellulosic bioenergy. Each *box* extends from the lower 25th to the 75th percentile with the median and mean shown as *solid* and *dashed* horizontal lines, respectively. *Upper* and *lower whiskers* indicate 10th and 90th percentiles. *Symbols* indicate 5th and 95th percentiles.

Future 2030. When compared with the no-CB-2030 landscape, nutrient concentrations and loadings simulated from CB-2030 landscapes decreased for the majority of subbasins (Table 2). Nitrate concentrations decreased in 90% of subbasins, with a median decrease of 4% (−0.05 mg L^{-1}). Nitrate loadings decreased in only 60% of subbasins (Fig. 5). Concentrations of TN decreased in 95% of subbasins, with a median decrease of 8.2% (−0.13 mg L^{-1}), and loadings decreased in 75% of subbasins (Fig. 5). Simulated TP concentrations decreased in 95% of subbasins, with a median decrease of 34.6% (−0.13 mg L^{-1}). TP loadings decreased in 80% of subbasins (Fig. 5).

Total suspended sediment concentrations increased in 70% of subbasins, with a median area-weighted change of 1.8% (+5.7 mg L^{-1}). However, sediment loadings decreased in 80% of subbasins and 90% of subbasins growing bioenergy crops. Median sediment loading calculated per-hectare-of-bioenergy decreased by 41.2%, suggesting that other factors played a role [e.g., shifts in nonbioenergy crops or in-stream contributions to TSS (i.e. reduced suspension of bedload sediment)]. Average flow decreased at the outlets of nearly all subbasins, with a median decrease of 13.7% (60.2 m^3 s^{-1}).

When weighted by area planted in bioenergy crops, median nutrient and sediment loadings decreased from No-CB-2030 levels for all analytes: −0.050 kg ha^{-1} NO3; −1.45 kg TN ha^{-1}; −0.041 kg ha^{-1} PO4; −0.724 kg TP ha^{-1}; and −208.6 kg sediment ha^{-1}. Median annual loadings weighted by total subbasin area in the No-CB-2030 scenario were 0.726 kg ha^{-1} NO3, 3.629 kg TN ha^{-1}, 0.755 kg TP ha^{-1}, 373.3 kg SYLD ha^{-1}, and 3,752 m^3 s^{-1} water.

Table 2 Projected median change (interquartile range) in water quality and quantity indicators from the no-CB baseline landscapes to those with bioenergy in future years 2022 or 2030. Changes that were consistently in one direction are in **bold**, changes for which the interquartile range bracketed zero are not. Concentrations are in the first row and loadings in the second row of each entry.

Water quality and quantity indicators, concentrations and loadings	Projected future bioenergy landscape	
	2022	2030
NO_3 (mg L^{-1})	+0.03 (−0.07 to +0.05)	**−0.05 (−0.08 to −0.03)**
NO_3 (kg ha^{-1})	−0.075 (−0.21 to +0.13)	−0.01 (−0.081 to +0.098)
TN (mg L^{-1})	+0.004 (−0.025 to +0.040)	**−0.13 (−0.25 to −0.09)**
TN (kg ha^{-1})	−0.35 (−0.96 to +0.05)	−0.203 (−0.885 to +0.003)
TP (mg L^{-1})	**−0.086 (−0.088 to −0.014)**	**−0.13 (−0.14 to −0.10)**
TP (kg ha^{-1})	**−0.145 (−0.374 to −0.017)**	**−0.13 (−0.453 to −0.017)**
TSS (mg L^{-1})	+5.48 (−0.519 to 92.5)	+5.7 (−5.2 to +25.1)
TSS (kg ha^{-1})	**−86.3 (−236 to −11)**	**−69.3 (−160.3 to −3.93)**
Flow (m^3 s^{-1})	**−79.4 (−85.9 to −9.8)**	**−60.2 (−142.9 to −12.6)**

Geographic variation. Soil Water Assessment Tool-simulated water quantity and quality attributes showed different spatial patterns of change between the pre- and postcellulosic scenarios for 2030 (Fig. 6). A general east-to-west pattern was evident for all four loadings (Fig. 6). Little-to-no change was evident in the western portion of the region, likely because no energy crops were predicted to grow there (see Fig. 2b). There was also very little change in the downstream, eastern portion of the Red River for sediment, TP, and TN (Fig. 6a, b, and d), but increases in nitrate (Fig. 6c). The largest decreases in loadings occurred in the longitudinal midsection for these three analytes (Fig. 6a, b, and d), regardless of river. Increases for all four analytes tended to occur in the Neosho-Verdigris basin in the north (Fig. 6). Nitrate showed a geographically different pattern from other analytes, with decreases tending to occur upstream and increases downstream. However, the Red River showed no change upstream (Fig. 6c).

Discussion

This study supports the idea that replacing annual with perennial crops can reduce TP (Banner *et al.*, 2009). Our simulations showed median decreases in nutrient and sediment loadings for the CB-2030 scenario compared with the No-CB-2030 baseline scenario with the same yield, tillage, and other management assumptions. Median water yield and flow at subbasin outlets also decreased in the CB-2030 scenario. However, when looking at concentrations, we see an increase in median values (Table 2). For sediment, TSS concentrations increased for both 2022 and 2030 (Table 2). Nitrogen variables showed a similar pattern in 2022, but not 2030. By 2030, simulated median changes were negative for both nitrate and TN (Table 2). Decreases in loadings accompanied by increases in concentration may be caused by decreased flow.

Geographically, subbasins varied in their responses; i.e. changes in nutrients and sediment increased in some

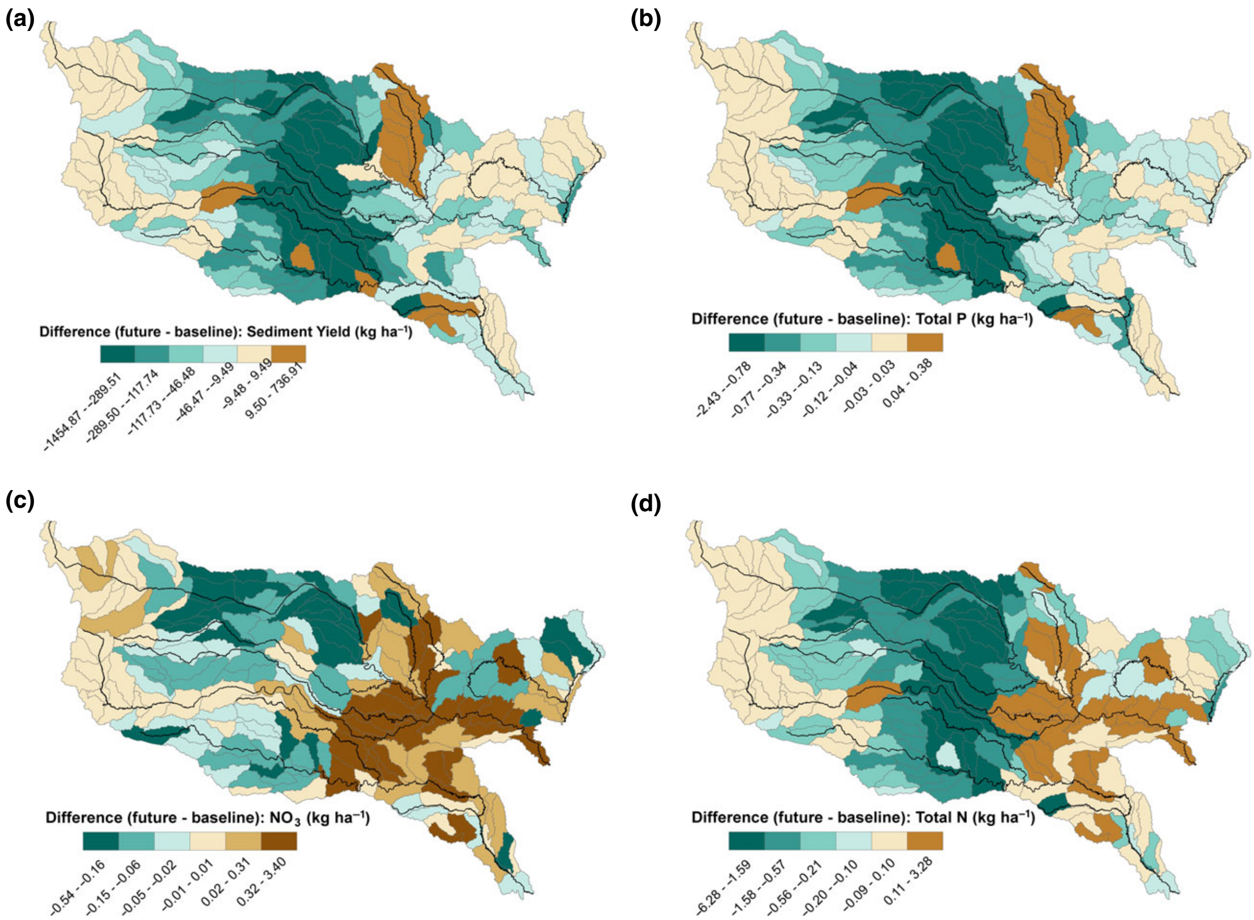

Fig. 6 Geographic distribution in change nutrient and sediment loadings between cellulosic bioenergy (CB) scenario and the no-cellulosic bioenergy scenario for 2030. Quantities reported are changes in yield for (a) sediment, (b) TP, (c) NO3, and (d) TN.

subbasins and decreased in others. However, simulated nutrient and sediment indicators always decreased when weighting each subbasin by area of bioenergy production (i.e. down-weighting subbasins with few or no bioenergy crops). In addition, water quality improvements were more widespread for the CB-2030 scenario than for the CB-2022 scenario, suggesting that conversion of more land is required to meet bioenergy-associated sustainability goals for improved water quality. This was particularly true for the two nitrogen variables.

Geographic variation in changes suggests that it would be more advantageous, from a water quality perspective, to convert to perennial energy crops between 97° and 100° longitude, rather than in subbasins farther east. The Neosho-Verdigris basin in the north (Fig. 2a) is one basin where increases were observed. In particular, nitrate increased downstream (major rivers run from the northwest to southeast). However, decreased TP and sediment loadings should help to alleviate water quality issues in highly agricultural areas of Arkansas and Kansas.

Improving water quality in AWR rivers can have far-reaching ecological consequences that extend from upstream watersheds where sediment and nutrient loadings occur to distant downstream reservoirs and estuaries (Howarth *et al.*, 2002). Upstream, in addition to the altered hydrologic regime, siltation and eutrophication are leading causes of fish and mussel extirpations in rivers and streams of the AWR drainage (Dodds & Oakes, 2004), as it is for the rest of North America (Richter *et al.*, 1997). In those subbasins where conversion of land to bioenergy feedstocks leads to improved water quality, the hope is for subsequent recovery of fishes (Schweizer & Jager, 2011) and other imperiled aquatic biota. However, the projected decreases in flow and future competing uses for water resources will continue to pose challenges for aquatic biota within the AWR (Muneepeerakul *et al.*, 2008). Downstream, nutrient loadings from the AWR drainage are a major contributor to seasonal hypoxia far downstream in the Gulf of Mexico (Alexander & Smith, 2006; Alexander *et al.*, 2008).

Not surprisingly, water quality outcomes were more promising for the AWR river basin than for prime agricultural lands to the north. A similar study to this one compared the implications of biofuel production in the Upper Mississippi River Basin (Demissie *et al.*, 2012) where corn stover is expected to be the dominant feedstock. One would expect the impacts of using corn or corn stover, grown with typical tillage practices and fertilizer application, to be comparable to those of growing corn for food. However, corn grown without tilling soil produces less runoff and loses less sediment than corn grown with tilling (Nyakatawa *et al.*, 2006). Demissie *et al.* (2012) simulated future landscapes consistent with projections of the 2022 Billion-Ton Update and observed increases in suspended sediment and total phosphorus, but decreases in total nitrogen loadings. All three water quality parameters increased when pasture or idle land was converted to corn and soybean grown for stover (Demissie *et al.*, 2012). Similar results were obtained for a smaller watershed within the Upper Mississippi river basin (Wu & Liu, 2012). However, nutrients and sediment decreased when improved bioenergy crops and better management practices were simulated (Wu *et al.*, 2012). Simulated improvements included higher nutrient efficiency in corn varieties, improved timing of fertilizer application, and reduced per-area stover removal for higher yielding varieties of corn.

Deep-rooted perennial switchgrass produces modest-to-high yields (Jager *et al.*, 2010) and could become economically feasible at relatively low cost where irrigation is not required (U.S. Department of Energy, 2011). Our results suggest that the middle band of the AWR river basin between 97° and 100° longitude is particularly promising for sustainable biomass production. Along this ecotone, precipitation starts to become limiting to both switchgrass and competing agricultural crops. However, agricultural crops require more irrigation water than switchgrass does and the source of irrigation water is the increasingly depleted Ogallala aquifer. We therefore expect switchgrass and other deep-rooted bioenergy feedstocks to find an economic niche where other water sources are not available (i.e. away from storage reservoirs and rivers).

In addition to economic sustainability, previous studies have suggested that perennial feedstocks such as switchgrass offer more environmentally benign alternatives to corn and crop residues (Nelson *et al.*, 2006; Love *et al.*, 2011; Powers *et al.*, 2011; Robertson *et al.*, 2011). However, concerns about bioenergy production and its effects on water quality persist (Gelfand *et al.*, 2013). Our study fills in this missing piece by addressing water quality implications for the AWR river basin. We identified subbasins at the intersection, where future economic feasibility and potential for water quality improvement are high, as well as less suitable areas. We conclude that parts of the AWR river basin hold promise for improving water quality through geographically judicious replacement of existing land uses with energy crops such as switchgrass.

Acknowledgements

This research was funded by the Department of Energy Bioenergy Technology Programs. Oak Ridge National Laboratory is managed by UT-Battelle, LLC for the U. S. Department of Energy under Contract No. DE-AC05-00OR22725. We thank Michelle Thornton (ORNL) for providing DAYMET data. In addition, we appreciate the insightful reviews of Dr. Gangsheng Wang and anonymous reviewers.

References

Alexander RB, Smith RA (2006) Trends in the nutrient enrichment of U.S. rivers during the late 20th century and their relation to changes in probable stream trophic conditions. *Limnology and Oceanography*, **5**, 639–654.

Alexander RB, Smith RA, Schwarz GE, Boyer EW, Nolan JV, Brakebill JW (2008) Differences in phosphorus and nitrogen delivery to the gulf of Mexico from the Mississippi river basin. *Environmental Science & Technology*, **42**, 822–830.

Allan JD (2004) Landscapes and riverscapes: the influence of land use on stream ecosystems. *Annual Review of Ecology and Evolutionary Sytematics*, **35**, 257–284.

Arnold JG, Kiniry JR, Srinivasan R, Williams JR, Haney EB, Neitsch SL (2012) *Soil & Water Assessment Tool Input/Output Documentation Version 2012*. (TR-439) Texas Water Resources Institute. Available at: http://twri.tamu.edu/reports/2013/tr439.pdf (accessed 31 January 2014).

Banner EBK, Stahl AJ, Dodds WK (2009) Stream discharge and riparian land use influence in-stream concentrations and loads of phosphorus from central plains watersheds. *Environmental Management*, **44**, 552–565.

Baskaran L, Jager HI, Schweizer PE, Srinivasan R (2010) Progress toward evaluating the sustainability of switchgrass as a bioenergy crop using the SWAT model. *Transactions of the American Society of Agricultural and Biological Engineers*, **53**, 1547–1556.

Baskaran LM, Jager HI, Srinivasan R, Turhollow AF Jr (2013) *Understanding Shifts in Agricultural Landscapes: Context Matters When Simulating Future Changes in Water Quantity and Quality*. Oak Ridge National Laboratory, ORNL/TM-2013/531. http://www.esd.ornl.gov/~zij/mypubs/Biofuels/BaskaranTM2013.pdf (accessed 02 February 2014).

Clark RB, Baligar VC, Zobel RW (2005) Response of mycorrhizal switchgrass to phosphorus fractions in acidic soil. *Communications in Soil Science and Plant Analysis*, **36**, 1337–1359.

De La Torre Ugarte D, Ray DE (2000) Biomass and bioenergy aplications of the POLYSYS modeling framework. *Biomass and Bioenergy*, **18**, 291–308.

Demissie Y, Yan E, Wu M (2012) Assessing regional hydrology and water quality implications of large-scale biofuel feedstock production in the Upper Mississippi river basin. *Environmental Science & Technology*, **46**, 9174–9182.

Dodds WK, Oakes RM (2004) A technique for establishing reference nutrient concentrations across watersheds affected by humans. *Limnology and Oceanography-Methods*, **2**, 333–341.

Dodds WK, Oakes RM (2008) Headwater influences on downstream water quality. *Environmental Management*, **41**, 367–377.

Donner SD, Kucharik CJ (2008) Corn-based ethanol production compromises goal of reducing nitrogen export by the Mississippi river. *Proceedings of the National Academy of Sciences of the United States of America*, **105**, 4513–4518.

Erickson JE, Woodard KR, Sollenberger LE (2012) Optimizing sweet sorghum production for biofuels in the southeastern USA through nitrogen fertilization and top removal. *Bioenergy Research*, **5**, 86–94.

Flueck WT, Smith-Flueck J, a. M., Monjeau J. A. (2011) Protected areas and extensive productions systems: a phosphorus challenge beyond human food. *BioScience*, **61**, 582–582.

Garten CT, Brice DJ, Castro HF, Graham RL, Mayes MA, Phillips JR, Smith JL (2011) Response of "Alamo" switchgrass tissue chemistry and biomass to nitrogen fertilization in west Tennessee, USA. *Agriculture Ecosystems & Environment*, **140**, 289–297.

Gassman PW, Reyes MR, Green CH, Arnold JG (2007) The soil and water assessment tool: historical development, applications, and future research directions. *Transactions of the American Society of Agricultural and Biological Engineers*, **50**, 1211–1250.

Gelfand I, Sahajpal R, Zhang XS, Izaurralde RC, Gross KL, Robertson GP (2013) Sustainable bioenergy production from marginal lands in the US midwest. *Nature*, **493**, 514–521.

Harmel D, Potter S, Casebolt P, Reckhow K, Green C, Haney R (2006) Compilation of measured nutrient load data for agricultural land uses in the United States. *Journal of the American Water Resources Association*, **42**, 1163–1178.

Horowitz J, Ebel R, Ueda K (2010) No-till farming is a growing practice. *Economic Information Bulletin*, **70**, 22.

Howarth RW, Sharpley A, Walker D (2002) Sources of nutrient pollution to coastal waters in the United States: implications for achieving coastal water quality goals. *Estuaries*, **25**, 656–676.

Hunsaker CT, Levine DA (1995) Hierarchical approaches to the study of water quality in rivers. *BioScience*, **45**, 193–203.

Jager HI, Baskaran LM, Brandt CC, Davis EB, Gunderson CA, Wullschleger SD (2010) Empirical geographic modeling of switchgrass yields in the United States. *Global Change Biology Bioenergy*, **2**, 248–257.

Johnson LB, Richards C, Host GE, Arthur JW (1997) Landscape influences on water chemistry in midwestern stream ecosystems. *Freshwater Biology*, **37**, 193–208.

Kiniry JR, Sanderson MA, Williams JR, Tischler CR, Hussey MA, Ocumpaugh WR, Reed RL (1996) Simulating alamo switchgrass with the ALMANAC model. *Agronomy Journal*, **88**, 602–606.

Kiniry JR, Cassida KA, Hussey MA *et al*. (2005) Switchgrass simulation by the ALMANAC model at diverse sites in the southern US. *Biomass and Bioenergy*, **29**, 419–425.

Langholtz M, Graham R, Eaton L, Perlack R, Hellwinkel C, De La Torre Ugarte D (2012) Price projections of feedstocks for biouels and biopower in the US. *Energy Policy*, **41**, 484–493.

Larson JA, English BC, Ugarte DGD (2008) An evaluation of the economic and environmental impacts of the corn grain ethanol industry on the agricultural sector. *Journal of Agricultural and Resource Economics*, **33**, 501–501.

Love BJ, Einheuser MD, Nejadhashemi AP (2011) Effects on aquatic and human health due to large scale bioenergy crop expansion. *Science of the Total Environment*, **409**, 3215–3229.

Maloney KO, Mulholland PJ, Feminella JW (2005a) Influence of catchment-scale military land use on stream physical and organic matter variables in small southeastern plains catchments (USA). *Environmental Management*, **35**, 677–691.

Maloney KO, Mulholland PJ, Feminella JW (2005b) ERRATUM: influence of catchment-scale military land use on stream physical and organic matter variables in small southeastern plain catchments (USA). *Environmental Management*, **36**, 918.

Muneepeerakul R, Bertuzzo E, Lynch HJ, Fagan WF, Rinaldo A, Rodriguiz-Iturbe I (2008) Neutral metacommunity models predict fish diversity patterns in Mississippi-Missouri basin. *Nature*, **453**, 220–229.

Musick JT, Pringle FB, Harman WL, Stewart BA (1990) Long-term irrigation trends: texas high plains. *Applied Engineering in Agriculture*, **6**, 717–724.

Nelson RG, Ascough JC, Langemeier MR (2006) Environmental and economic analysis of switchgrass production for water quality improvement in northeast Kansas. *Journal of Environmental Management*, **79**, 336–347.

Nyakatawa EZ, Mays DA, Tolbert VR, Green TH, Bingham L (2006) Runoff, sediment, nitrogen, and phosphorus losses from agricultural land converted to sweetgum and switchgrass bioenergy feedstock production in north Alabama. *Biomass and Bioenergy*, **30**, 655–664.

Parton WJ, Gutmann MP, Ojima D (2007) Long-term trends in population, farm income, and crop production in the Great Plains. *BioScience*, **57**, 737–747.

Powers SE, Ascough JC, Nelson RG, Larocque GR (2011) Modeling water and soil quality environmental impacts associated with bioenergy crop production and biomass removal in the midwest USA. *Ecological Modelling*, **222**, 2430–2447.

Richter BD, David P, Braun Michael A, Mendelson Master L L (1997) Threats to imperiled freshwater fauna. *Conservation Biology*, **11**, 1081–1093.

Robertson GP, Hamilton SK, Del Grosso SJ, Parton WJ (2011) The biogeochemistry of bioenergy landscapes: carbon, nitrogen, and water considerations. *Ecological Applications*, **21**, 1055–1067.

Samson F, Knopf F (1994) Prairie conservation in North America. *BioScience*, **44**, 418–421.

Sanderson MA, Jones RM, Mcfarland MJ, Stroup J, Reed RL, Muir JP (2001) Nutrient movement and removal in a switchgrass biomass-filter strip system treated with dairy manure. *Journal of Environmental Quality*, **30**, 210–216.

Scanlon BR, Faunt CC, Longuevergne L, Reedy RC, Alley WM, Mcguire VL, Mcmahon PB (2012) Groundwater depletion and sustainability of irrigation in the US high plains and Central Valley. *Proceedings of the National Academy of Sciences of the United States of America*, **109**, 9320–9325.

Schweizer PE, Jager HI (2011) Modeling regional variation in riverine fish biodiversity in the Arkansas-White-Red river basin. *Transactions of the American Fisheries Society*, **140**, 1227–1239.

Soil Survey Staff (1994) *U.S. General Soil Map (STATSGO)*. Natural Resources Conservation Service, Washington, D.C.

Srinivasan R, Zhang X, Arnold J (2010) SWAT ungauged: hydrological budget and crop yield predictions in the Upper Mississippi river basin. *Transactions of the American Society of Agricultural and Biological Engineers*, **53**, 1533–1546.

Thornton PE, Running SW, White MA (1997) Generating surfaces of daily meteorology variables over large regions of complex terrain. *Journal of Hydrology*, **190**, 214–251.

Uri N (2000) Perceptions on the use of no-till farming in production agriculture in the United States: an analysis of survey results. *Agriculture, Ecosystems and Environment*, **77**, 263–266.

U.S. Department of Agriculture (1997) Agricultural Handbook Number 628. Available at: http://usda01.library.cornell.edu/usda/nass/planting//1990s/1997/planting-12-05-1997.pdf (accessed 31 January 2014).

U.S. Department of Agriculture (2009) NASS Statistics 2009-2010. Available at: http://www.nass.usda.gov/QuickStats/ (accessed 31 January 2014).

U.S. Department of Energy (2011) *U.S. Billion-Ton Update: Biomass Supply for a Bioenergy and Bioproducts Industry* (eds Perlack RD, Stokes BJ), p. 122. Oak Ridge National Laboratory, Oak Ridge, TN.

Venuto B, Kindiger B (2008) Forage and biomass feedstock production from hybrid forage sorghum and sorghum-sudangrass hybrids. *Journal of Japanese Society of Grassland Science*, **54**, 189–196.

White M. (2006) *Predicted Sweet Sorghum Yields in Oklahoma by Soil and Climate Region*. Oklahoma State University and US Department of Agriculture Agricultural Research Service, Available at: http://www.ars.usda.gov/SP2UserFiles/ad_hoc/62060505MikeWhite/pdfs/Sorghum7-25-2006.pdf (accessed 31 January 2014).

Wu YP, Liu SG (2012) Impacts of biofuels production alternatives on water quantity and quality in the Iowa river basin. *Biomass and Bioenergy*, **36**, 182–191.

Wu M, Demissie Y, Yan E (2012) Simulated impact of future biofuel production on water quality and water cycle dynamics in the Upper Mississippi river basin. *Biomass and Bioenergy*, **41**, 44–56.